



## THERMOELECTRIC PROPERTIES OF CoRhYSi (Y = Cr, Mn) QHA.

Mr. Sameer Ahmad Pala, Dr Veeresh Kumar

PHD Research Scholar in Department of Physics, Sunrise University Alwar, Rajasthan – 301026  
Assistant Professor in Department of Physics at Sunrise University, Alwar Rajasthan – 301026  
[Vks8361@gmail.com](mailto:Vks8361@gmail.com)

---

### ABSTRACT

Thermoelectric materials have potential properties for utilizing waste heat. The computations are used to estimate the electronic structure of CoRhYSi (Y = Cr, Mn) Quaternary Heusler alloys, as well as their elastic and magnetic characteristics. The full-potential linearized augmented plane wave is used in the calculations. The exchange-correlations are addressed using Perdew–Burke and Ernzerhof's generalized gradient approximation (GGA-PBE). With the exception of CoRhCrSi and CoRhMnSi, which are simple ferromagnets that are approximately half metallic in nature, electronic structure calculations demonstrate that these compounds have a gap in the minority states band and are obviously half-metallic ferromagnets. The magnetic moments of the CoRhCrSi and CoRhMnSi compounds match relatively well with the Slater-Pauling rule, indicating half metallicity and high spin polarization for these compounds. The semi-classical Boltzmann theory was used to compute the Seebeck coefficient (S), electrical conductivity ( $\sigma$ ), and electronic thermal conductivity ( $k_e$ ) of CoRhYSi (Y = Cr, Mn) alloys, whereas Slack's equation was used to get the lattice thermal conductivity ( $k_L$ ).

**KEYWORDS:-** Thermoelectric properties, Seebeck coefficient (S), electrical conductivity ( $\sigma$ ), and electronic thermal conductivity ( $k_e$ ), Debye Temperature.

---

**DOI: 10.48047/ecb/2022.11.11.27**

### INTRODUCTION

The increasing demands for fossil fuels due the vast leap in technology has urged the search for other alternative sources of energy. In addition, the intensive use of fossil fuels for most of public transport and industrial production created other problems such as pollution and global climate change. Regarding the energy consumption, the waste heat is one of the problems,

where 75% of energy consumption is in the form of thermal energy, and the mechanical power utilizes only 25% of the energy [1], [2]. Therefore, scientists have been searching for other alternative resources that have a sustainability and can use this waste of heat. One of these resources is the thermoelectric generators, which are renewable and environmentally friendly source of energy that can transform waste heat to electricity [3].

The thermoelectric devices are composed of p- and n-type of semiconductors that are connected electrically in series and thermally in parallel. On one hand, they can operate as thermal generators of voltage as a result of temperature gradient between the two sides of the thermoelectric modules in a phenomenon known as the Seebeck effect [4] (Figure 1a). On the other hand, they can be used in refrigeration, where the heat transfers from one side to the other side of the module by applying an electric current in a phenomenon known as Peltier effect [5] (Figure 1b). Thermoelectric materials have become one of the most promising resources of energy owing to the low cost of production, the eco-friendly electricity generation, the sustainability, fewer moving parts and less maintenance. Thermoelectric materials have been very successful in transforming waste heat into electricity in several applications such as radioisotope thermoelectric generators in NASA's spacecrafts [6]. The research in this field was focused on application such as geometry, cooling, shape, size, and also the adaptation of the heat flow of systems [7]–[9].

Heusler alloys are promising materials for thermoelectric applications. There are several properties that make Heusler alloys interesting such as half metallicity, ferromagnetism, spin gapless semiconducting, superconductivity, semiconducting, and shape memory effect [10]–[13].

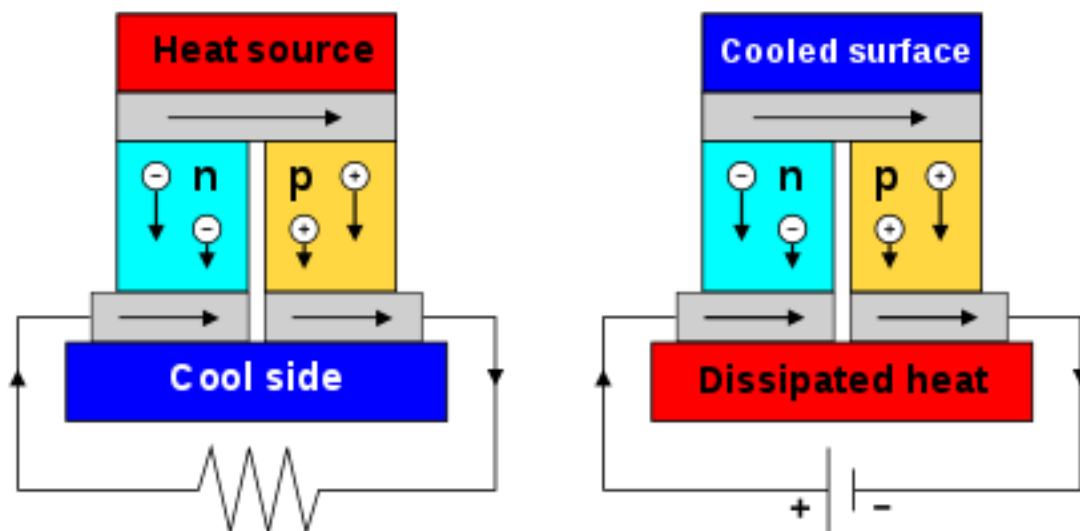


**Figure 1. (a) Seebeck effect thermocouple. (b) Peltier effect thermocouple.**

## COMPUTATIONAL METHOD

Density functional theory (DFT), as implemented in VASP code is used to do the calculations. TE properties were calculated using DFT with a high-density mesh of 10,000 k-points, which is equivalent to a 36 x 36 x 36 centered k-mesh. The constant relaxation time approximation was used for the TE computations, which was set to  $0.5 \times 10^{-15}$  s.

## THERMOELECTRIC PROPERTIES

By using the Boltzmann transport theory with constant relaxation time approximation, the thermoelectric properties of CoRhYSi (Y = Mn, Cr) quaternary Heusler compounds were examined [14], [15]. Predicting the electronic transport properties by this method of approximation showed good results comparing with the experimental measurements [12]–[19]. To calculate the thermoelectric properties, the constant relaxation time of  $\tau \sim 0.5 \times 10^{-15}$  s was used. Similar systems, such as FeRhCrSi and FeRhCrGe QHAs, were also examined [20]. When the materials have a narrow band gap, they could have a great efficiency to transform the heat to electricity [21]. These alloys were observed to have small band gaps of 0.542 eV and 0.576 eV in the majority spin channel, making them particularly promising for thermoelectric applications. A semiconductor with a narrow band gap is assumed to have high thermoelectric properties [22]–[24]. The Seebeck coefficient ( $S$ ) and the electrical conductivity ( $\sigma$ ) are depending in the spin in the half-metallic material.

The following equations are used to compute the Seebeck coefficient ( $S$ ), electrical conductivity ( $\sigma$ ), and electronic thermal conductivity ( $k_e$ ) [25]:

$$\sigma_{\alpha\beta}(T, \mu) = \frac{1}{\Omega} \int \sigma_{\alpha\beta}(\epsilon) \left[ -\frac{\partial f_{\mu}(T, \epsilon)}{\partial \epsilon} \right] d\epsilon$$

$$k_{\alpha\beta}(T, \mu) = \frac{1}{e^2 T \Omega} \int \sigma_{\alpha\beta}(\epsilon) (\epsilon - \mu)^2 \left[ -\frac{\partial f_{\mu}(T, \epsilon)}{\partial \epsilon} \right] d\epsilon$$

$$S_{\alpha\beta}(T, \mu) = \frac{1}{e T \Omega \sigma_{\alpha\beta}(T, \mu)} \int \sigma_{\alpha\beta}(\epsilon) (\epsilon - \mu) \left[ -\frac{\partial f_{\mu}(T, \epsilon)}{\partial \epsilon} \right] d\epsilon$$

$$\sigma_{\alpha\beta} = \frac{e^2}{N_k} \sum_{i,k} \tau v_{\alpha}(i, k) v_{\beta}(i, k) \frac{\delta(\epsilon - \epsilon_{i,k})}{d\epsilon}$$

Where  $\sigma$  is the electrical conductivity,  $k_e$  is the electric thermal conductivity,  $S$  is the Seebeck coefficient,  $\alpha$  and  $\beta$  are tensor components, and  $\Omega$ ,  $v$ , and  $N_k$  are the chemical potential.

The total Seebeck coefficient and electrical conductivity of the majority and minority spin channels were calculated using the two-current model, as shown in [26]:

$$S = (S_{\uparrow}\sigma_{\uparrow} + S_{\downarrow}\sigma_{\downarrow})/\sigma_{\uparrow} + \sigma_{\downarrow}$$

Where ( $\uparrow$ ) and ( $\downarrow$ ) are the spin-up and spin-down channels, and the  $\sigma_{total}$  is the total electrical conductivity that is written as [26]:

$$\sigma_{total} = (\sigma_{\uparrow} + \sigma_{\downarrow})$$

The Seebeck coefficient of spin-up and spin-down channels and the total S as a function of the chemical potential at 300 K and 800 K show in Figure 2 (a), (b). The total Seebeck coefficient values increase as the temperature goes up, as can be seen in this graph. The highest values of S for the CoCrRhSi and CoMnRhSi alloys are achieved at 800 K, with values of 7.86976  $\mu V/K$  and 37.6746  $\mu V/K$ , respectively. At 300 K and 800 K, Figure 2 (c), (d) shows the electrical conductivity ( $\sigma$ ) as a function of the chemical potential. The electrical conductivity of the n-type is found to be higher than that of the p-type. Furthermore, the impact of temperature on values is shown to be minimal. Additionally, Figure 2 (c), (d) indicates that  $k_e$  behaves similarly to  $\sigma$  (n-type  $k_e$  values are higher than p-type  $k_e$  values). The direct relationship between electrical conductivity and electronic thermal conductivity ( $k_e$ ), which is approximated by the Wiedemann–Franz equation ( $k_e = L\sigma T$ ) is responsible for this [14]. Therefore, as the temperature goes up, the  $k_e$  values increase as well. The power factor (PF) is shown in Fig. 2 (e), (f), with the values increasing as the temperature increases. At 800 K, the maximum PF values for CoCrRhSi and CoMnRhSi alloys are  $20.2596 \times 10^{11}$ , and  $31.1445 \times 10^{11} \text{ Wm}^{-1}\text{K}^{-2}$ , respectively. The lattice thermal conductivity (kl) of the investigated alloys was computed using Slack's equation, which is one of the most accurate techniques for computing kl value, as follows [27]–[30]:

$$K_l = A \frac{\bar{M}\Theta_D^3 V^{1/3}}{\gamma^2 n^{2/3} T}$$

$$A = \frac{2.43 \times 10^{-6}}{1 - \frac{0.514}{\gamma} + \frac{0.228}{\gamma^2}}$$

Where A,  $\bar{M}$ ,  $\Theta_D$ , V,  $\gamma$ , n, T and T are the average atomic mass, Debye temperature, volume per atom, Grüneisen parameter, number of atoms in the primitive unit cell, and temperature, respectively [30]. The Debye temperature and the Grüneisen parameter are derived using the

following formulae based on the elastic constant computations [30], [31]:

$$\Theta_D = \frac{h}{k_B} \left( \frac{3n\rho N_A}{4\pi M} \right)^{1/3} v_m$$

$$v_m = \left[ \frac{1}{3} \left( \frac{2}{v_t^3} + \frac{1}{v_l^2} \right) \right]^{-1/3}$$

$$v_t = \sqrt{\frac{G}{\rho}}$$

$$\gamma = \frac{9 - 12(v_t/v_l)^2}{2 + 4(v_t/v_l)^2}$$

The Planck constant, density, Avogadro's number, Boltzmann constant, and molecular weight are represented by the constants  $h$ ,  $\rho$ ,  $N_A$ ,  $k_B$ , and  $M$ , respectively, whereas  $v_m$ ,  $v_l$ , and

$v_t$  are the average, transverse, and longitudinal sound velocities, respectively. Table 1 shows that

the Debye temperatures of CoCrRhSi and CoMnRhSi alloys are 420.78573K, and 454.28902 K, respectively. This table shows that decreasing the average sound velocities lowers the Debye temperature, which is consistent with previous computations by Co<sub>2</sub>MnAl, Co<sub>2</sub>MnGa, and Co<sub>2</sub>MnIn [32]. A high Debye temperature indicates that the material is hard, whereas low values are noticeable in soft materials [33].

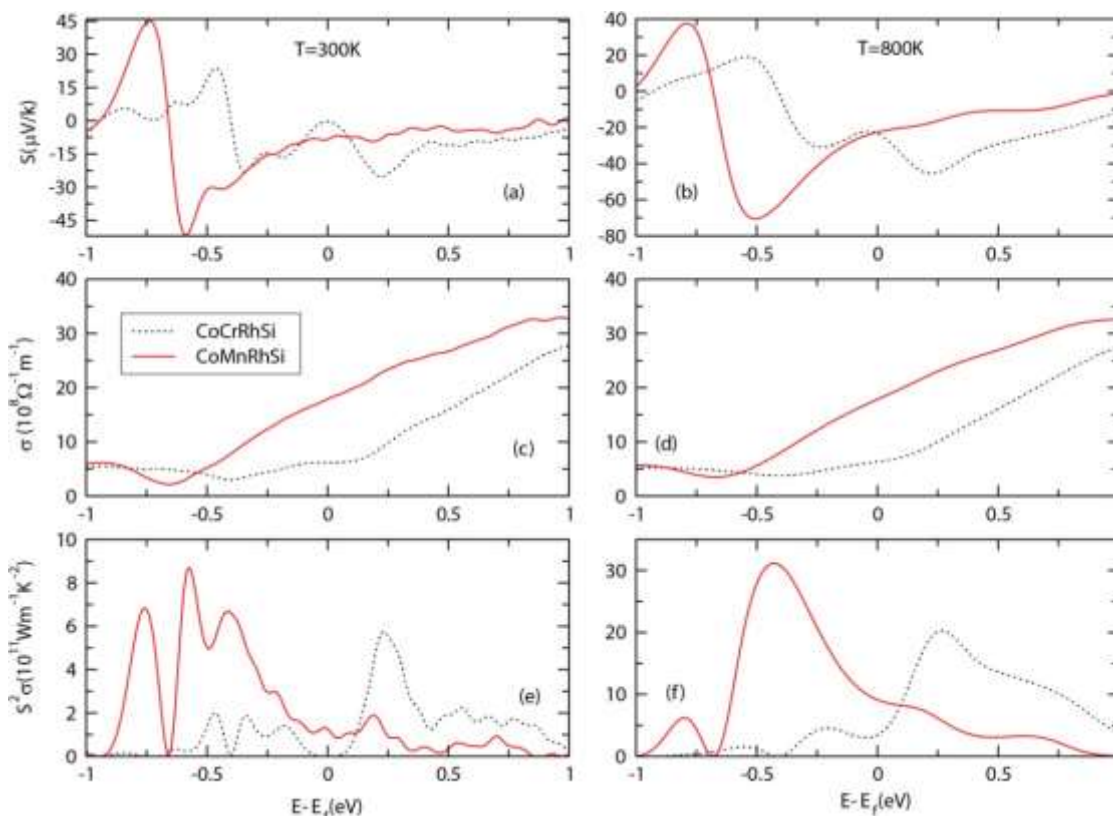


**Figure 2.** a, b the Seebeck coefficient ( $S$ ), c, d electrical conductivity ( $\sigma$ ), and e, f power factor PF ( $S^2\sigma$ ) as a function of the chemical potential at temperatures of (300 K, 800 K) for CoRhYSi(Y = Mn, Cr) QHAs.

**Table 1.** The Debye temperature  $\Theta_D$  (K), average sound velocity  $v_m$  (m/s), transverse sound velocity  $v_t$  (m/s), longitudinal sound velocity  $v_l$  (m/s), density  $\rho$  (kg/m<sup>3</sup>), and Grüneisen parameter  $\gamma$  for CoRhYSi (Y = Mn, Cr) QHAs.

Alloys	$\Theta_D$	$v_m$	$v_t$	$v_l$	$\rho$	$\gamma$
CoCrRhSi	420.78573	3274.84773	2909.84588	6176.90820	8186.08620	2.19
CoMnRhSi	454.28902	3533.46082	3151.32506	6250.75660	8073.10299	1.97

Using the aforementioned values, the lattice thermal conductivity ( $K_l$ ) was calculated (see Figure 3). The lattice thermal conductivity of CoRhYSi (Y = Mn, Cr) alloys declines as temperature rises, as seen in this graph. At 300 K, the lattice thermal conductivity of CoCrRhSi and CoMnRhSi is 1.84065 and 2.95174  $Wm^{-1}K^{-1}$ , respectively, and at 800 K, the lattice thermal conductivity of CoCrRhSi and CoMnRhSi is 0.690245 and 1.1069

$Wm^{-1}K^{-1}$ , respectively. At 300 K, these values are lower than related structures like CoFeCrGe ( $11.01Wm^{-1}K^{-2}$ ) and CoFeTiGe ( $12.26 Wm^{-1}K^{-2}$ ) [34]. Figure 4 shows the figure of merit ZT values as a function of chemical potential at 300 and 800 K. At 800 K, CoRhYSi (Y = Mn, Cr) alloys have greater ZT values, as shown in this figure 3. At 800 K, CoCrRhSi and CoMnRhSi have the highest n-type ZT values of 0.838235 and 2.04368 eV, respectively. These ZT values are greater than recent calculations of 0.45 eV and 0.41 eV for FeRhCrSi and FeRhCrGe QHAs, respectively, at 800 K [20].

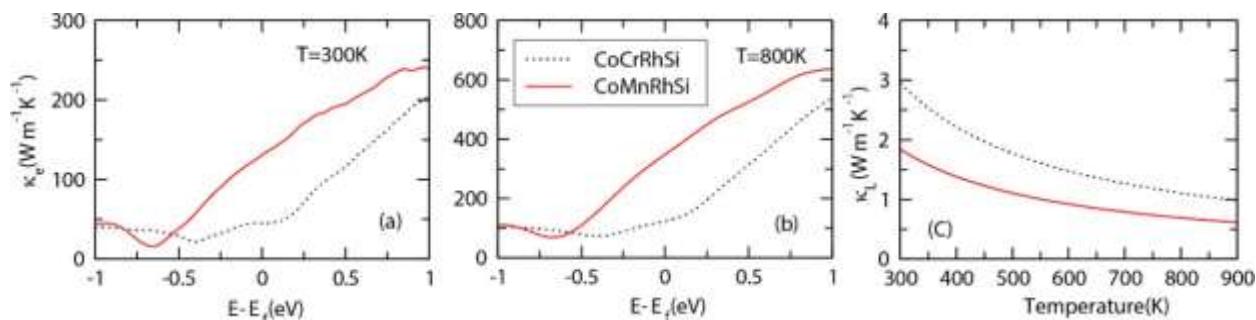


**Figure 3. a, b electronic thermal conductivity ( $\kappa_e$ ) and the lattice thermal conductivity ( $\kappa_l$ ) as a function of the temperature for CoRhYSi (Y = Mn, Cr) as a function of the chemical potential at (300 K, 800 K) for CoRhYSi (Y = Mn, Cr) alloys**

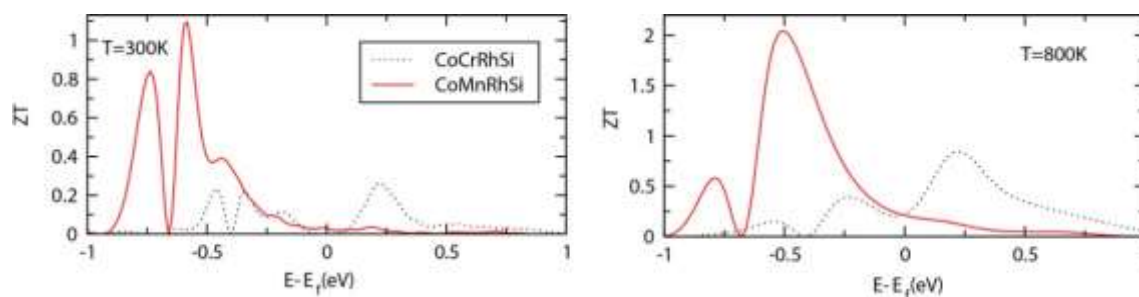


**Figure 4. the figure of merit (ZT) as a function of the chemical potential at (300 K, 800 K) for CoRhYSi (Y = Mn, Cr) alloys**

## CONCLUSION

. CoRhYSi (Y = Mn, Cr) QHAs are calculated to have good thermoelectric properties using the constant relaxation time approach of the semi-classical Boltzmann transport theory. The maximal power factors for CoCrRhSi and CoMnRhSi QHAs at 800 K are  $20.2596 \times 10^{11}$  and  $31.1445 \times 10^{11} Wm^{-1}K^{-2}$ , respectively. The calculations predict that n-type CoCrRhSi and CoMnRhSi have the highest ZT values of 0.84 and 2.04, respectively, whereas CoMnRhSi has the highest p-type ZT value of 2.04 at 800 K. As a



result, these alloys have the potential to be used in thermoelectric applications at high temperatures.

## Acknowledgement

I want to thank everyone involved in this initiative. I'd like to thank my supervisor and mentor Dr Veeresh Kumar Department of Physics at Sunrise University, Alwar Rajasthan, who helped me learn a lot about this project. His ideas and comments aided in completion of this research paper.

## REFERENCES

- [1] C. Haddad, C. Périlhon, A. Danlos, M.-X. François, and G. Descombes, "Some efficient solutions to recover low and medium waste heat: competitiveness of the thermoacoustic technology," *Energy Procedia*, vol. 50, pp. 1056–1069, 2014.
- [2] J. Yang and F. R. Stabler, "Automotive applications of thermoelectric materials," *J. Electron. Mater.*, vol. 38, no. 7, p. 1245, 2009.
- [3] L. E. Bell, "Cooling, heating, generating power, and recovering waste heat with thermoelectric systems," *Science*, vol. 321, no. 5895, pp. 1457–1461, 2008.
- [4] J. R. Sootsman, D. Y. Chung, and M. G. Kanatzidis, "New and old concepts in thermoelectric materials," *Angew. Chem. Int. Ed.*, vol. 48, no. 46, pp. 8616–8639, 2009.
- [5] A. Montecucco, J. Buckle, and A. Knox, "Solution to the 1-D unsteady heat conduction equation with internal Joule heat generation for thermoelectric devices," *Appl. Therm. Eng.*, vol. 35, pp. 177–184, 2012.
- [6] J. Yang and T. Caillat, "Thermoelectric materials for space and automotive power generation," *MRS Bull.*, vol. 31, no. 3, pp. 224–229, 2006.
- [7] R. Goldstein *et al.*, "Heat transfer—A review of 2004 literature," *Int. J. Heat Mass Transf.*, vol. 53, no. 21–22, pp. 4343–4396, 2010.
- [8] X. Liu, C. Li, Y. Deng, and C. Su, "An energy-harvesting system using thermoelectric power generation for automotive application," *Int. J. Electr. Power Energy Syst.*, vol. 67, pp. 510–516, 2015.
- [9] Z. Liu, C. Davis, W. Cai, L. He, X. Chen, and H. Dai, "Circulation and long-term fate of functionalized, biocompatible single-walled carbon nanotubes in mice probed by Raman spectroscopy," *Proc. Natl. Acad. Sci.*, vol. 105, no. 5, pp. 1410–1415, 2008.
- [10] C. Felser, G. H. Fecher, and B. Balke, "Spintronics: a challenge for materials science and solid-state chemistry," *Angew. Chem. Int. Ed.*, vol. 46, no. 5, pp. 668–

699, 2007.

- [11] D. Jung, H.-J. Koo, and M.-H. Whangbo, "Study of the 18-electron band gap and ferromagnetism in semi-Heusler compounds by non-spin-polarized electronic band structure calculations," *J. Mol. Struct. THEOCHEM*, vol. 527, no. 1–3, pp. 113–119, 2000.
- [12] K. Özdoğan, E. Şaşıoğlu, and I. Galanakis, "Slater-Pauling behavior in LiMgPdSn-type multifunctional quaternary Heusler materials: Half-metallicity, spin-gapless and magnetic semiconductors," *J. Appl. Phys.*, vol. 113, no. 19, p. 193903, 2013.
- [13] Y. Sutou *et al.*, "Magnetic and martensitic transformations of NiMnX (X= In, Sn, Sb) ferromagnetic shape memory alloys," *Appl. Phys. Lett.*, vol. 85, no. 19, pp. 4358–4360, 2004.
- [14] H. Alqurashi and B. Hamad, "Magnetic structure, mechanical stability and thermoelectric properties of VTiRhZ (Z= Si, Ge, Sn) quaternary Heusler alloys: first-principles calculations," *Appl. Phys. A*, vol. 127, no. 10, pp. 1–11, 2021.
- [15] M. Geilhufe *et al.*, "Effect of hydrostatic pressure and uniaxial strain on the electronic structure of  $Pb_{1-x}Sn_xTe$ ," *Phys. Rev. B*, vol. 92, no. 23, p. 235203, 2015.
- [16] L. Xi *et al.*, "Chemical bonding, conductive network, and thermoelectric performance of the ternary semiconductors  $Cu_2SnX_3$  (X= Se, S) from first principles," *Phys. Rev. B*, vol. 86, no. 15, p. 155201, 2012.
- [17] D. Parker and D. J. Singh, "High-temperature thermoelectric performance of heavily doped PbSe," *Phys. Rev. B*, vol. 82, no. 3, p. 035204, 2010.
- [18] H. Wang, W. Chu, and H. Jin, "Theoretical study on thermoelectric properties of  $Mg_2Si$  and comparison to experiments," *Comput. Mater. Sci.*, vol. 60, pp. 224–230, 2012.
- [19] T. Thonhauser, T. Scheidemantel, J. Sofo, J. Badding, and G. Mahan, "Thermoelectric properties of  $Sb_2Te_3$  under pressure and uniaxial stress," *Phys. Rev. B*, vol. 68, no. 8, p. 085201, 2003.
- [20] S. A. Khandy and J.-D. Chai, "Thermoelectric properties, phonon, and mechanical stability of new half-metallic quaternary Heusler alloys:  $FeRhCrZ$  (Z= Si and Ge)," *J. Appl. Phys.*, vol. 127, no. 16, p. 165102, 2020.
- [21] G. Mahan and J. Sofo, "The best thermoelectric," *Proc. Natl. Acad. Sci.*, vol. 93, no. 15, pp. 7436–7439, 1996.
- [22] J. O. Sofo and G. Mahan, "Optimum band gap of a thermoelectric material," *Phys. Rev. B*, vol. 49, no. 7, p. 4565, 1994.
- [23] Z. M. Gibbs, H.-S. Kim, H. Wang, and G. J. Snyder, "Band gap estimation from temperature dependent Seebeck measurement—Deviations from the  $2e|S| \max T_{max}$  relation," *Appl. Phys. Lett.*, vol. 106, no. 2, p. 022112, 2015.

- [24] E. H. Hasdeo, L. P. Krisna, M. Y. Hanna, B. E. Gunara, N. T. Hung, and A. R. Nugraha, "Optimal band gap for improved thermoelectric performance of two-dimensional Dirac materials," *J. Appl. Phys.*, vol. 126, no. 3, p. 035109, 2019.
- [25] T. Lin, Q. Gao, G. Liu, X. Dai, X. Zhang, and H. Zhang, "Dynamical stability, electronic and thermoelectric properties of quaternary ZnFeTiSi Heusler compound," *Curr. Appl. Phys.*, vol. 19, no. 6, pp. 721–727, 2019.
- [26] S. Singh and D. C. Gupta, "Lanthanum based quaternary Heusler alloys LaCoCrX (X = Al, Ga): Hunt for half-metallicity and high thermoelectric efficiency," *Results Phys.*, vol. 13, p. 102300, 2019.
- [27] A. Hong *et al.*, "Full-scale computation for all the thermoelectric property parameters of half-Heusler compounds," *Sci. Rep.*, vol. 6, no. 1, pp. 1–12, 2016.
- [28] H. Ma, C.-L. Yang, M.-S. Wang, X.-G. Ma, and Y.-G. Yi, "Effect of M elements (M = Ti, Zr, and Hf) on thermoelectric performance of the half-Heusler compounds MCoBi," *J. Phys. Appl. Phys.*, vol. 52, no. 25, p. 255501, 2019.
- [29] R. Haleoot and B. Hamad, "Thermoelectric properties of doped  $\beta$ -InSe by Bi: first principle calculations," *Phys. B Condens. Matter*, vol. 587, p. 412105, 2020.
- [30] G. A. Slack, "Nonmetallic crystals with high thermal conductivity," *J. Phys. Chem. Solids*, vol. 34, no. 2, pp. 321–335, 1973.
- [31] C. Li and Z. Wang, "Computational modelling and ab initio calculations in MAX phases-I," *Adv. Sci. Technol. Mn MAXn Phases*, pp. 197–222, 2012.
- [32] S.C. Wu, G. H. Fecher, S. Shahab Naghavi, and C. Felser, "Elastic properties and stability of Heusler compounds: Cubic Co<sub>2</sub>YZ compounds with L 21 structure," *J. Appl. Phys.*, vol. 125, no. 8, p. 082523, 2019.
- [33] D. Hoat *et al.*, "First principles analysis of the half-metallic ferromagnetism, elastic and thermodynamic properties of equiatomic quaternary Heusler compound CoCrRhSi," *Mater. Chem. Phys.*, vol. 257, p. 123695, 2021.
- [34] R. Haleoot and B. Hamad, "Thermodynamic and thermoelectric properties of CoFeYGe (Y = Ti, Cr) quaternary Heusler alloys: first principle calculations," *J. Phys. Condens. Matter*, vol. 32, no. 7, p. 075402, 2019.